The Journal of Anatomical Sciences
Email: journalofanatomicalsciences@gmail.com

J. Anat Sci 17(2) June

Submitted: April 17th, 2026
Revised: June 11th, 2026
Accepted: June 24th, 2026

Effects of Ethanol Leaf Extract of *Chromolaena odorata* on the Hippocampus of Alloxan-induced Diabetic Wistar Rats Exposed to Mercuric Chloride

Monday Nelly Chima*[1]; Njoku Clinton Ogbonnaya[2]; Albert Eteudo N; Ama, Ifeanyichukwu Maxwell[3]; Uche, Vincent Uchenna[4]

Department of Anatomy, Ebonyi State University, Abakaliki, Ebonyi State, Nigeria

ORCID number: [1]0009-0006-4794-0712; [2]0000-0001-6082-9177; [3]0009-0000-3449-393X; [4]0009-0007-6924-0159.

***Corresponding Author:** Email: chimamonday87@gmail.com

ABSTRACT

Diabetes mellitus and mercury toxicity are associated with oxidative stress and neuronal degeneration, particularly in the hippocampus. The study assessed histological and immunohistochemical effects of ethanol leaf extract of *Chromolaena odorata* on the hippocampus of alloxan-induced diabetic Wistar albino rats exposed to mercuric chloride. Thirty-six adult Wistar rats were randomly assigned to six groups. Diabetes was induced using alloxan monohydrate (150mg/kg), while mercury toxicity was induced using mercuric chloride (3mg/kg). Treatment groups received graded doses of *Chromolaena odorata* extract at 200, 400, and 600 mg/kg and metformin (standard drug). Biochemical assays for oxidative stress markers, including malondialdehyde, superoxide dismutase, glutathione peroxidase, histological evaluation, and immunohistochemical analyses (GFAP and p53) were carried out. Significant elevation in malondialdehyde level (910.59±32.73) and reduction in antioxidant enzymes (SOD: 21.04±2.30; GPx: 37.78±6.20) were observed in untreated diabetic rats exposed to mercury compared to controls. Treatment with *Chromolaena odorata* extract significantly reduced MDA level and restored antioxidant enzyme activity. Histological findings showed neuronal degeneration in CA1, CA3, and dentate gyrus regions in untreated rats, while treated groups showed preserved neuronal architecture. Immunohistochemistry revealed increased GFAP and p53 expression in untreated groups, which were reduced following treatment. Ethanol leaf extract of *Chromolaena odorata* exhibits significant neuroprotective and antioxidant effects against diabetes and mercury-induced hippocampal damage.

Keywords: *Chromolaena odorata*, hippocampus, diabetes mellitus, mercuric chloride, GFAP, p53, oxidative stress

INTRODUCTION

A chronic metabolic disorder such as diabetes mellitus (DM) is characterized by a persistent high blood glucose level, which results from impaired insulin secretion, defective insulin action, or both mechanisms occurring simultaneously [1]. It is a global health challenge affecting populations in both developed and developing nations. The prevalence of diabetes mellitus has increased significantly in recent decades due to urbanization, reduced physical exercise, aging populations, and unhealthy dietary habits. Approximately 537 million adults were living with diabetes globally, with projections indicating a substantial increase in future years [2].

Chronic diabetes is associated with several complications involving multiple organs: the cardiovascular system, kidneys, retina, peripheral nerves, and the brain. Sustained hyperglycemia promotes oxidative stress, inflammatory responses, and metabolic imbalance, which contribute to progressive tissue injury and dysfunction [3]. Increasing evidence suggests that diabetes-related complications extend beyond peripheral organs to the central nervous system, where it is associated with cognitive decline, structural brain abnormalities, and increased susceptibility to neurodegenerative disorders [4].

Alloxan is a toxic glucose analogue and among the commonly employed diabetogenic agents. It is capable of destroying β-cells in the pancreas selectively through reactive oxygen species-mediated mechanisms, thereby causing insulin deficiency and persistent hyperglycemia [5]. Experimental studies using alloxan-induced diabetic models have provided useful information regarding the biochemical,

metabolic, and histopathological alterations associated with diabetes and to evaluate potential therapeutic interventions.

Oxidative stress results when there is an imbalance in the generation of reactive oxygen species (ROS) and antioxidant defense level in the body [6]. In diabetes, chronic hyperglycemia enhances ROS production through glucose autoxidation, dysfunction of the mitochondrial and polyol pathway activation [7].

The brain is particularly susceptible to oxidative damage due to its high oxygen demand, abundant lipids, and relatively poor antioxidant defense system. The hippocampus is specifically vulnerable to oxidative injury. This structure plays important roles in learning, memory processing, and emotional regulation [8]. Consequently, structural or functional impairment of the hippocampus may result in memory deficits and cognitive dysfunction observed in several neurological disorders.

Apart from metabolic disturbances, environmental toxicants have also contributed to the development of neurotoxicity. Mercury, a toxic heavy metal, is widely distributed through natural and environmental activities such as mining operations, industrial emissions, and improper disposal of wastes [9]. Inorganic mercury compounds induce oxidative stress, inflammatory responses, mitochondrial dysfunction, and neuronal degeneration [10]. Following exposure, mercury may cross the blood-brain barrier and accumulate within neural tissues, interfere with cellular metabolism, and promote neurotoxicity. The hippocampus region is particularly vulnerable to mercury-induced damage due to its high metabolic activities and sensitivity to oxidative injury, [11].

Experimental evidence has demonstrated that chronic exposure to inorganic mercury may impair learning and memory and produce biochemical and structural alterations within the hippocampus [10]. Previous studies reported that oxidative stress, disruption of calcium homeostasis, and impairment of endogenous antioxidant defense mechanisms are associated with mercury-induced neurotoxicity.

Interest in medicinal plants as potential therapeutic agents for diabetes and its complications has increased considerably in recent years. Herbal remedies remain widely utilized in many parts of the world because of their accessibility, affordability, and long-term use in traditional medicine. Traditional medicine plays an important role in healthcare delivery globally [12].

Chromolaena odorata (Siam weed), of the family of Asteraceae, distributed across tropical and subtropical regions, is traditionally used in the management of wounds, infections, inflammation, and metabolic disorders [13]. The plant contains several bioactive constituents, including flavonoids, phenolic compounds, terpenoids, and alkaloids known for antioxidant and neuroprotective activities [14]. Bioactive flavonoids such as quercetin, luteolin, and kaempferol possess free radical scavenging properties, which may enhance endogenous antioxidant enzyme activity.

Previous investigations reported antidiabetic, antimicrobial, anti-inflammatory, and hepatoprotective properties of *Chromolaena odorata*[15]. However, its neuroprotective potential under conditions involving both diabetes and mercury-induced neurotoxicity remains inadequately explored. Therefore, the study investigated histological and immunohistochemical effects of *chromolaena odorata* ethanol leaf extract on the hippocampus of alloxan-induced diabetic Wistar albino rats exposed to mercuric chloride.

MATERIALS AND METHODS

Experimental animals

The thirty-six adult Wistar albino rats aged 12–16 weeks, weighing 200 g, were purchased from the animal house of the department of Anatomy, Ebonyi State University, Abakaliki.

The animals were housed in the wire-gauze plastic cages with sawdust bedding, and maintained under standard laboratory and environmental conditions with a natural 12:12 hours light and dark cycle. The rats were fed with standard grower's mash and water ad libitum. They were acclimatized for one week.

The choice of using male rats was to eliminate hormonal fluctuations associated with the estrous cycle in female rats, which may influence biochemical, histological, and immunohistochemical outcomes.

Chemical and reagents

The chemicals and reagents used in the study were of analytical grade. Alloxan monohydrate and mercuric chloride were obtained from Zayo-Sigma Chemicals Ltd., Jos, Nigeria (a partner distributor of Sigma-Aldrich Chemical Company. Biochemical assay kits were obtained from Randox Laboratories Ltd, Atlas Medical Diagnostics Ltd, and Agappe Diagnostics Switzerland. Metformin was purchased from Octovia Pharmacy in Abakaliki, Ebonyi State. Alloxan (150 mg/kg) and mercury chloride (3 mg/kg/day) solutions were freshly prepared in normal saline, respectively.

Ethical consideration

The procedures adopted in the study were in accordance with the guidelines for laboratory animal care and the Institutional Animal Care and Use Committee (IACUC). Ethical approval was procured from the Research and Ethics Committee of the Faculty of Basic Medical Sciences, Ebonyi State University, with Ethical Code: MPC/2502/30/013.

Plant identification and extraction

Fresh leaves of *Chromolaena odorata* were collected in the Ebonyi State University Premises at the Presco Campus. The leaves were identified by Professor C. V. Nnamani (a qualified taxonomist) in the

University's herbarium. The leaves were washed with distilled water, defoliated, and shade-dried for 10 days to prevent degradation of heat-Labile constituents. The dried leaves were ground into powder form using a mortar and pestle. One hundred grams of the powder form was soaked in a liter of 70% ethanol for 72 hours with vigorous shaking to ensure efficient extraction.

The mixture was filtered with a filter paper, and the ethanol evaporated, leaving behind the extract that was used for the study, followed by further drying in a water bath to remove residual solvent. The dried extract, hereafter referred to as extract (COLE), was stored in the refrigerator at 4°C. During administration, the extract was reconstituted in distilled water and given to experimental animals according to their individual body weights and assigned dose groups such that the maximum volume administered to each rat did not exceed 0.5 ml.

Experimental design

A randomized controlled experimental design was used. After a week of acclimatization, the animals were weighed and randomly separated into six (6) groups of six (6) animals each, as seen in Table 1**.** Induction of diabetes in groups B-F using a single intraperitoneal injection of 150 mg/kg of alloxan monohydrate. Blood samples collected from the tail vein after 72 hours of alloxan administration were used to measure fasting blood glucose levels by the use of glucometer. The animals with fasting blood glucose of 200 mg/dL and above were considered diabetic.

Mercury toxicity was induced using intraperitoneal injection of 3 mg/kg of mercuric chloride for 14 days. Treatment with *Chromolaena odorata* extract and metformin commenced on the third day of mercuric chloride administration and continued for 14 days.

Normal control (group A) received 0.1ml of normal saline (0.9% NaCl) orally for 28 days. Group B (diabetic rats exposed to inorganic mercury) received a single intraperitoneal (IP) injection of 150 mg/kg of alloxan monohydrate dissolved in normal saline to induce type 1 diabetes mellitus, followed by administration of 3 mg/kg of mercuric chloride. Group C (COLE-200) (diabetic rats exposed to inorganic mercury) received a single intraperitoneal (IP) injection of 150 mg/kg of alloxan monohydrate, followed by administration of 3 mg/kg body weight mercuric chloride, and subsequently treated with 200 mg/kg of *Chromolaena odorata* leaf extract (COLE) for 14 days (low dose). Group D (COLE-400); (diabetic rats exposed to inorganic mercury) received a single intraperitoneal (IP) injection of 150 mg/kg of alloxan monohydrate, followed by administration of 3 mg/kg of mercuric chloride, and subsequently treated with 400 mg/kg of *Chromolaena odorata* leaf extract (COLE) for 14 days (medium dose). Group E (COLE-600); (diabetic rats exposed to inorganic mercury) received a single intraperitoneal (IP) injection of 150 mg/kg of alloxan monohydrate, followed by administration of 3 mg/kg of mercuric chloride, and subsequently treated orally with 600 mg/kg of *Chromolaena odorata* leaf extract (COLE) for 14 days (high dose). Group F (Metformin), diabetic and mercury-exposed rats treated with metformin hydrochloride at 500 mg/kg for 14 days (standard drug). The extract doses were adopted and modified from [16], while the metformin dose was based on [17]. The selected doses of *Chromolaena odorata* extract were based on previous studies that demonstrated the safety and therapeutic efficacy of the extract within the administered dose range.

Table 1: Experimental grouping and treatment protocol

Groups	Alloxan Mercury Chloride (Day12–25)	Treatment (Day15–28)
Control	No	Distilled water
Diabetic + Mercury Toxicity	Yes	No treatment
Diabetic + Mercury + C. odorata (Low dose)	Yes	Low dose extract
Diabetic + Mercury + C. odorata (Medium dose)	Yes	Medium dose extract
Diabetic + Mercury + C. odorata (High dose)	Yes	High dose extract
Diabetic + Mercury + Standard drug	Yes	Metformin

Histological processing

The brain tissues were fixed in neutral buffered formalin for histological processing. The fixed tissues were dehydrated in graded ethanol solutions, cleared in xylene, embedded in paraffin wax, and sectioned at 5 µm using a rotary microtome. The sections were mounted onto positively charged slides, stained with Hematoxylin and Eosin (H&E), and examined microscopically to evaluate the hippocampal histoarchitecture [18]. Photomicrographs were obtained using an Amscope research microscope at the Biotechnology Research Center, Ebonyi State University, Abakaliki.

Immunohistochemistry

The Immunohistochemical staining for GFAP and p53 was performed using the avidin-biotin peroxidase technique. The embedded sections cut at 4 µm thick were mounted on positively charged slides, deparaffinized, and rehydrated through descending grades of ethanol. The antigen retrieval was performed in citrate buffer at pH 6.0 using microwave heating. Endogenous peroxidase activity was blocked with 3% hydrogen peroxide, while nonspecific binding was prevented using normal goat serum. The sections were incubated in primary antibodies against GFAP (1:100) and p53 (1:80) and biotinylated goat anti-rabbit secondary antibodies. Visualization was done using diaminobenzidine (DAB) chromogen, and the slides were counterstained with Mayer's hematoxylin. Positive immunoreactivity.

Biochemical assays

Lipid peroxidation was assessed by measuring malondialdehyde (MDA), while antioxidant enzyme activities such as superoxide dismutase (SOD) and glutathione peroxidase (GPx) were determined using standard spectrophotometric methods.

Morphometric analysis

From each group, six non-overlapping high-power fields at a magnification of ×400 from the immunohistochemically-stained sections of GFAP and p53 were morphometrically analyzed using Image J analyzer software. The percentage area of GFAP staining and the number of p53-positive cells (pyramidal cell layer) were calculated and quantified from non-overlapping high-power fields.

Statistical analysis

The raw data obtained were analyzed using one-way analysis of variance (ANOVA) and Tukey post-hoc multiple comparison test using Statistical Package for Social Sciences (SPSS) version 25. Differences were considered statistically significant at 0.05. The data were expressed as Mean ± SEM.

RESULTS

Oxidative stress markers in hippocampal tissue

Malondialdehyde levels are presented in Table 2 and Figure 1. Group B recorded a significant increase in malondialdehyde (MDA) level compared to the normal control. Treatment with ethanol extract of *Chromolaena odorata* significantly reduced the MDA levels in groups C, D, and E respectively, compared to group B. Group F showed comparable reductions in MDA levels approaching the values observed in the normal control group.

Superoxide Dismutase (SOD)levels are presented in Table 2 and Figure 2**.** Superoxide Dismutase activity significantly decreased in group B with $p < 0.05$ compared to the normal control group. However, Treatment with *Chromolaena odorata* extract significantly increased SOD activity in groups C, D, and E respectively. Group F also showed improvement in SOD levels. The increase in SOD level indicated restoration of antioxidant defense close to the normal control group.

Glutathione Peroxidase **(**GPx) levels are presented in Table 2 and Figure 3. The result showed a significant decrease inGPx activity in Group B with $p < 0.05$ compared to the normal control group. Treatment with ethanol leaf extract of *Chromolaena odorata* significantly increased GPx activity in groups C, D, and E respectively. Groups F demonstrated increases in GPx levels.

Effect of *Chromolaena odorata* on hippocampal histoarchitecture

The normal control showed the Cornu Ammonis (CA) with its different sub-regions and the dentate gyrus (DG). Each sub-region of CA1 and CA3 presented three layers: the polymorphic layer (POL), which contains glial cell nuclei, the pyramidal cell layer (PCL), which encloses pyramidal cells that appeared small and compacted in CA1 and large and loosely packed in CA3, and the molecular layer (ML), which contains glial cells and apical dendrites of the pyramidal cells. There was scanty cytoplasm and large, rounded nuclei with prominent nucleoli in the pyramidal cells of the pyramidal cell layer, stratum lucidum, which forms a narrow zone, was seen only in CA3. The molecular, granule cell (GCL), and polymorphic layers of the dentate gyrus were present. Alveus, and the hippocampal sulcus which separates the Cornu Ammonis from the DG were also seen. (b): showed three layers of CA1 in high magnification of the boxed area in the inset; POL displayed deeply-stained (ds) and lightly-stained (ls) glial nuclei, PCL has pyramidal cells with large, rounded vesicular nuclei and prominent nucleoli. ML revealed ds and ls glial nuclei and blood vessels. (c): showed the wing of the three layers of CA3 in high magnification of the boxed area in the inset. POL displays ls and ds glial cell nuclei. The Stratum Lucidum layer is seen. There were pyramidal cells with large, rounded nuclei and scanty cytoplasm in PCL. Perineural glial cells and apical dendrite (bifid arrow) were also noticed. Molecular layer exhibits Is and ds nuclei of glial cells.

The untreated diabetic group showed disruption of the layers in CA1 and CA3. POL displayed deeply stained glial cell nuclei and dilated blood vessels. Presence of shrunken pyramidal cells with deeply stained elongated nuclei in PCL. Perineural glial cells were seen around the degenerated pyramidal cells. Many deeply and lightly stained glial cell nuclei in the ML. In addition, CA3 displayed disrupted fibers of SL.

Table 2: Malondialdehyde, superoxide dismutase, and glutathione peroxidase levels

Group	MDA (nmol/mg Protein)	SOD (U/mg Protein)	GPx (U/mgProtein)
Control	478.62 ± 13.08	33.60 ± 2.70	60.85 ± 2.19
Untreated diabetic	910.59 ± 32.73*	21.04 ± 2.30*	37.78 ± 6.20*
Extract 200 mg/kg(low dose)	644.06 ± 32.29*#	27.77 ± 1.80*#	55.48 ± 2.28*#
Extract 400 mg/kg(medium dose)	657.20 ± 13.90*#	27.62 ± 3.02*#	55.72 ± 2.70*#
Extract 600 mg/kg(high dose)	554.62 ± 16.13#	32.18 ± 2.50#	60.21 ± 2.03#
Metformin	555.63 ± 17.14#	33.19 ± 3.51#	61.22 ± 6.21#

The data were analyzed using one-way ANOVA and the Tukey post-hoc multiple comparison test. The p-value at < 0.05 is significant when compared to the normal control; # p value significant when compared to group B.

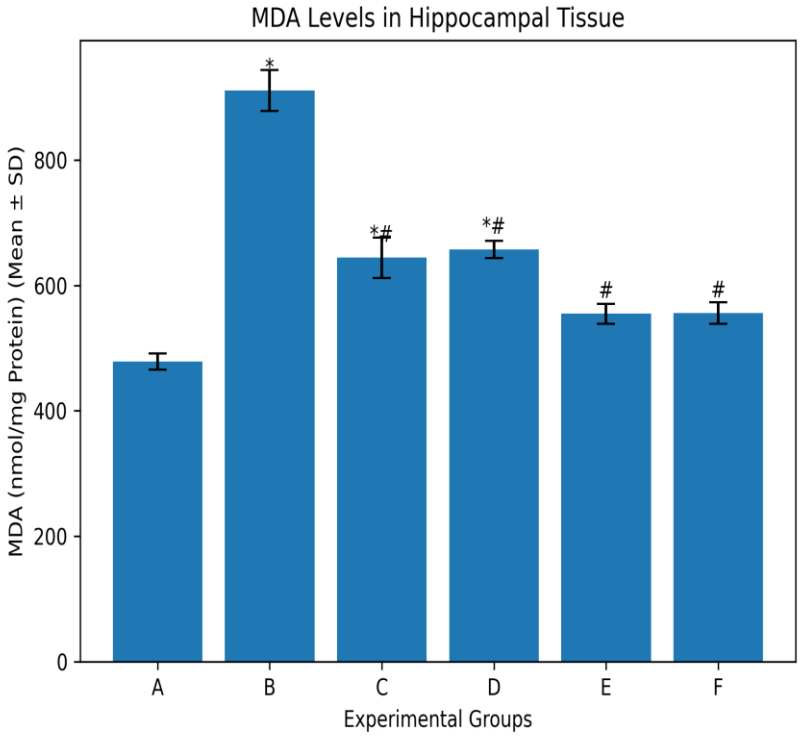

Figure 1: Effect of *Chromolaena odorata* extract on malondialdehyde (MDA) level in treatment groups. The p-value at < 0.05 is significant when compared to the normal control; # p value significant when compared to group B. (A): Control, (B): Alloxan + $HgCl_2$. (C): Alloxan + $HgCl_2$ +*Chromolaena odorata* extract (200 mg/kg), (D): Alloxan + $HgCl_2$ +*Chromolaena odorata* extract (400 mg/kg), (E): Alloxan + $HgCl_2$ +*Chromolaena odorata* extract (600 mg/kg), and (F): Alloxan + $HgCl_2$ + Metformin.

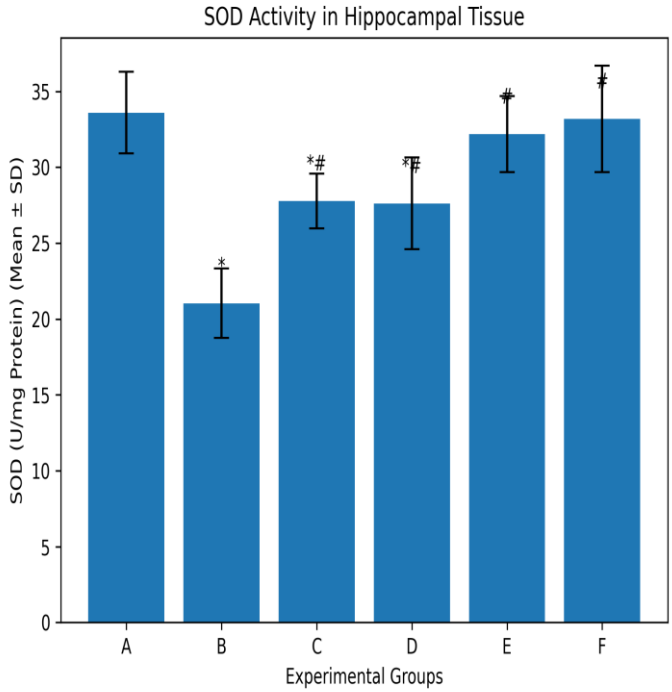

Figure 2: Effect of *Chromolaena odorata* extract on superoxide dismutase (SOD) level in treatment groups. The p-value at < 0.05 is significant when compared to the control group; $^{\#}$p value significant when compared to group B. (A): Control, (B): Alloxan + $HgCl_2$. (C): Alloxan + $HgCl_2$ +*Chromolaena odorata* extract (200 mg/kg), (D): Alloxan + $HgCl_2$ +*Chromolaena odorata* extract (400 mg/kg), (E): Alloxan + $HgCl_2$ +*Chromolaena odorata* extract (600 mg/kg), and (F): Alloxan + $HgCl_2$ + Metformin.

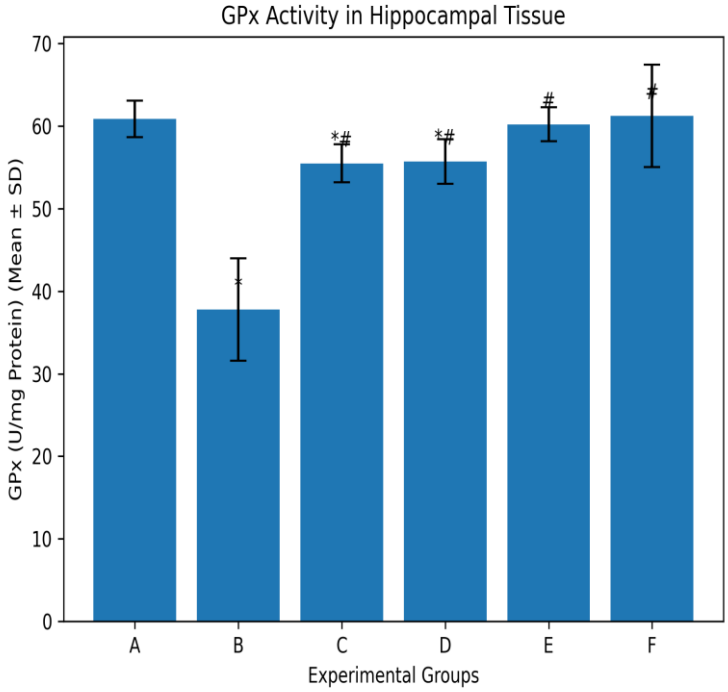

Figure 3: Effect of *Chromolaena odorata* extract on glutathione peroxidase (GPx) level in treatment groups. The p-value at < 0.05 is significant when compared to the control group; $^{\#}$p value significant when compared to group B. (A): Control, (B): Alloxan + $HgCl_2$. (C): Alloxan + $HgCl_2$ +*Chromolaena odorata* extract (200 mg/kg), (D): Alloxan + $HgCl_2$ +*Chromolaena odorata* extract (400 mg/kg), (E): Alloxan + $HgCl_2$ +*Chromolaena odorata* extract (600 mg/kg), and (F): Alloxan + $HgCl_2$ + Metformin.

It showed all the sub-regions of the Cornu Ammonis, DG, HS, and a dilated lateral ventricle with the choroid plexus. (b): showed CA1 with its three layers in high magnification of the boxed area in the inset: POL has deeply stained glial cell nuclei and dilated blood vessels. There are deeply stained, elongated nuclei (pn) in most cells of PCL; some pyramidal cells have large, lightly stained normal nuclei. Perineural glial cell nuclei can be observed around the degenerated neurons (curved arrow). ML revealed deeply and lightly stained nuclei. (c)High magnification of the boxed area in the inset of CA3 showed the stratum lucidum with its disrupted fibers. Most pyramidal cells were disturbed and degenerated with shrunken, deeply stained, elongated nuclei (curved arrow) with pericellular vacuolation in the PCL. Scanty pyramidal cells with large, lightly stained normal nuclei are seen, lightly stained glial nuclei with wide pericellular space in ML, while POL exhibits deeply stained nuclei of glial cells.

The CA1 and CA3 of the extract-treated group C exhibited deeply and lightly stained glial cell nuclei with a wide pericellular halo in POL. (a): Most pyramidal cells appeared normal, while a few cells were degenerated with deeply shrunken, elongated nuclei in PCL. There were deeply and lightly stained glial cell nuclei with a wide pericellular space in ML. (a): The paramedian section showed DG, CA1, CA2, CA3, CA4 and HS. (b): High magnification of the boxed area in the inset showed wing CA1 with its layers; lightly stained nuclei with wide pericellular haloes in POL. There are apparently normal pyramidal cells and a few degenerated cells with deeply stained, shrunken, elongated, and pyknotic nuclei in the PCL. ML exhibited deep and light-stained glial cell nuclei. (c): The high magnification of the boxed area in the inset showed CA3. Deeply stained nuclei with wide pericellular spaces in CML. PCL reveals that most pyramidal cells are apparently normal with lightly stained cytoplasm, and a few cells degenerated, having pyknotic nuclei with pericellular vacuolation. Stratum lucidum appears slightly disturbed. There was a slightly dilated blood vessel, ds and ls glial cells nuclei in the polymorphic layer.

The Cornu Ammonis 1 and 3 of the extract-treated group D showed deeply and lightly stained glial cell nuclei with a wide pericellular halo alongside dilated blood vessels in POL. (a): Apparently, normal pyramidal cells together with a few cells degenerated in PCL. ML revealed many glial cell nuclei with a wide pericellular space. (a): the paramedian section showed DG, CA1, CA2, CA3, CA4 and HS. (b): High magnification of the boxed area in the inset showed CA1; POL has deeply stained nuclei with a wide pericellular space. There were normal pyramidal cells with few degenerated cells having deeply stained, shrunken, elongated pyknotic nuclei with pericellular vacuolation in PCL. ML has lightly stained and deeply stained glial cell nuclei. (c): High magnification of the boxed area in the inset showed CA3 and stratum lucidum. lightly stained and deeply stained glial cell nuclei with a wide pericellular space seen in ML. Most pyramidal cells in PCL appeared normal, while a few cells were degenerated, having pyknotic nuclei with pericellular vacuolation. POL exhibits a blood vessel with a perivascular space.

The CA1 and CA3 of the extract-treated group E displayed normal POL, PCL contained apparently normal pyramidal cells with large, rounded vesicular nuclei and prominent nucleoli. Lightly stained and darkly stained glial cells with little pericellular space in ML. (a): the paramedian section showed DG, CA1, CA2, CA3, CA4 and HS. (b): The high magnification of the boxed area in the inset showed CA1. PCL exhibited normal pyramidal cells with large, rounded vesicular nuclei and prominent nucleoli, while a few cells had dark shrunk nuclei (arrow). There were lightly and darkly stained glial cell nuclei with little pericellular spaces and blood vessels in the molecular layer. (c): High magnification of the boxed area in the inset showed the layers of CA3; POL, PCL have normal pyramidal cells with large, rounded vesicular nuclei and prominent nucleoli, normal SL, and darkly stained glial nuclei with apparently normal blood vessels in ML.

The Cornu Ammonis 1 and 3 of the metformin-treated group F displayed normal POL, apparently normal pyramidal cells with large, rounded vesicular nuclei and prominent nucleoli in PCL. ML showed lightly stained and darkly stained glial cells with little pericellular space. (a): the paramedian section showed DG, CA1, CA2, CA3, CA4 and HS. (b): high magnification of the boxed area in the inset showed the three layers of CA1. PCL exhibited normal pyramidal cells with large, rounded vesicular nuclei and prominent nucleoli, with a few cells having dark, shrunken nuclei. The molecular layer has lightly and darkly stained glial cell nuclei with few pericellular spaces and blood vessels. (c): High magnification of the boxed area in the inset showed the layers of CA3; POL, PCL displays normal pyramidal cells with large, rounded vesicular nuclei and prominent nucleoli, normal SL and ML having darkly stained glial nuclei with apparently normal blood vessels.

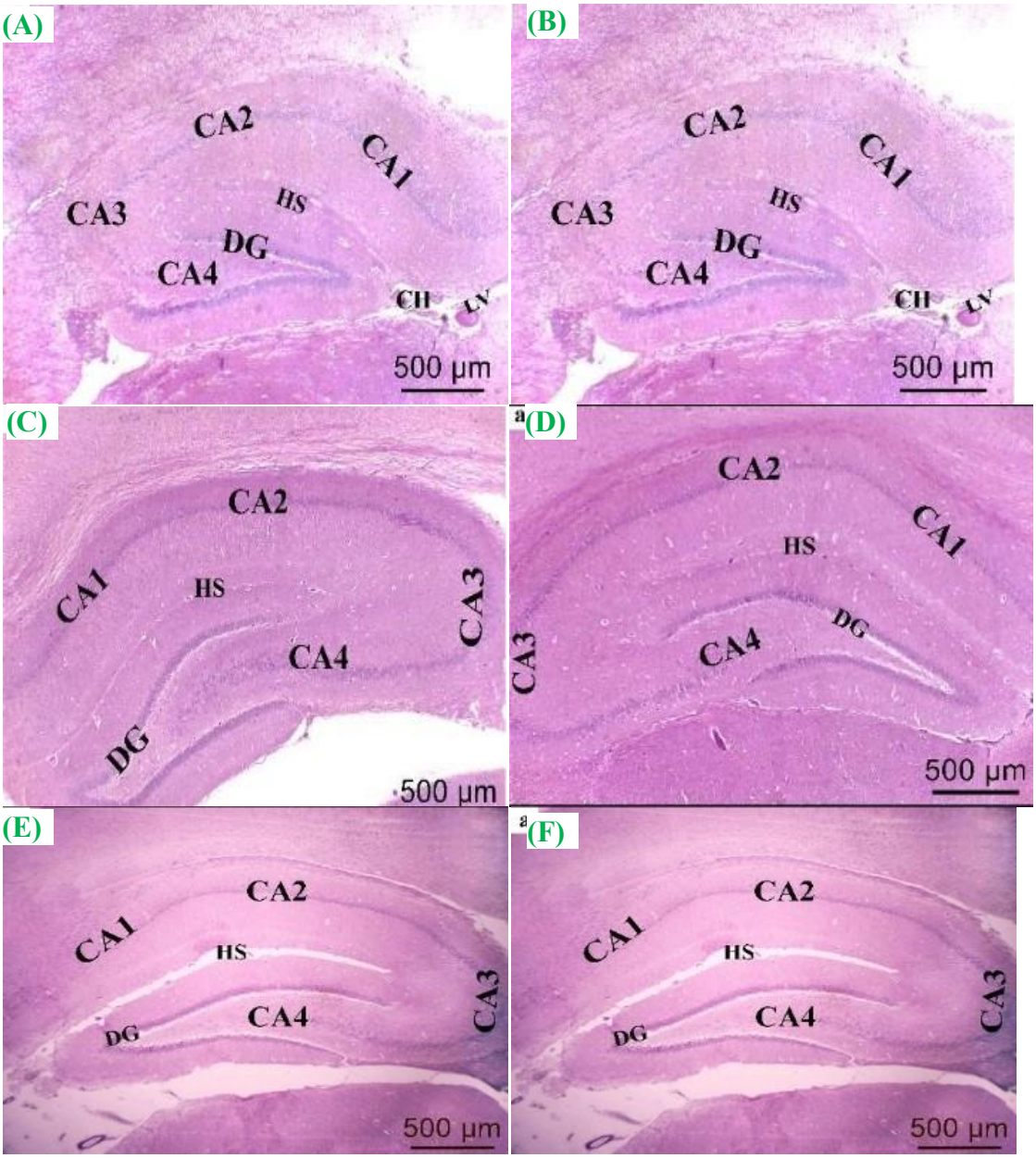

Figure 4: Photomicrographs of H&E-stained hippocampal sections in Control (A), Alloxan + $HgCl_2$ (B), Alloxan + $HgCl_2$ + *Chromolaena odorata* extract 200 mg/kg (C), Alloxan + $HgCl_2$ + *Chromolaena odorata* extract 400 mg/kg (D), Alloxan + $HgCl_2$ + *Chromolaena odorata* extract 600 mg/kg (E), and Alloxan + $HgCl_2$ + Metformin (F). The control group demonstrated normal hippocampal cytoarchitecture with well-arranged pyramidal neurons. Group B showed marked neuronal degeneration (pyknotic nuclei), disrupted neuronal arrangement, vacuolation, and gliosis, while treatment groups demonstrated varying degrees of structural preservation.

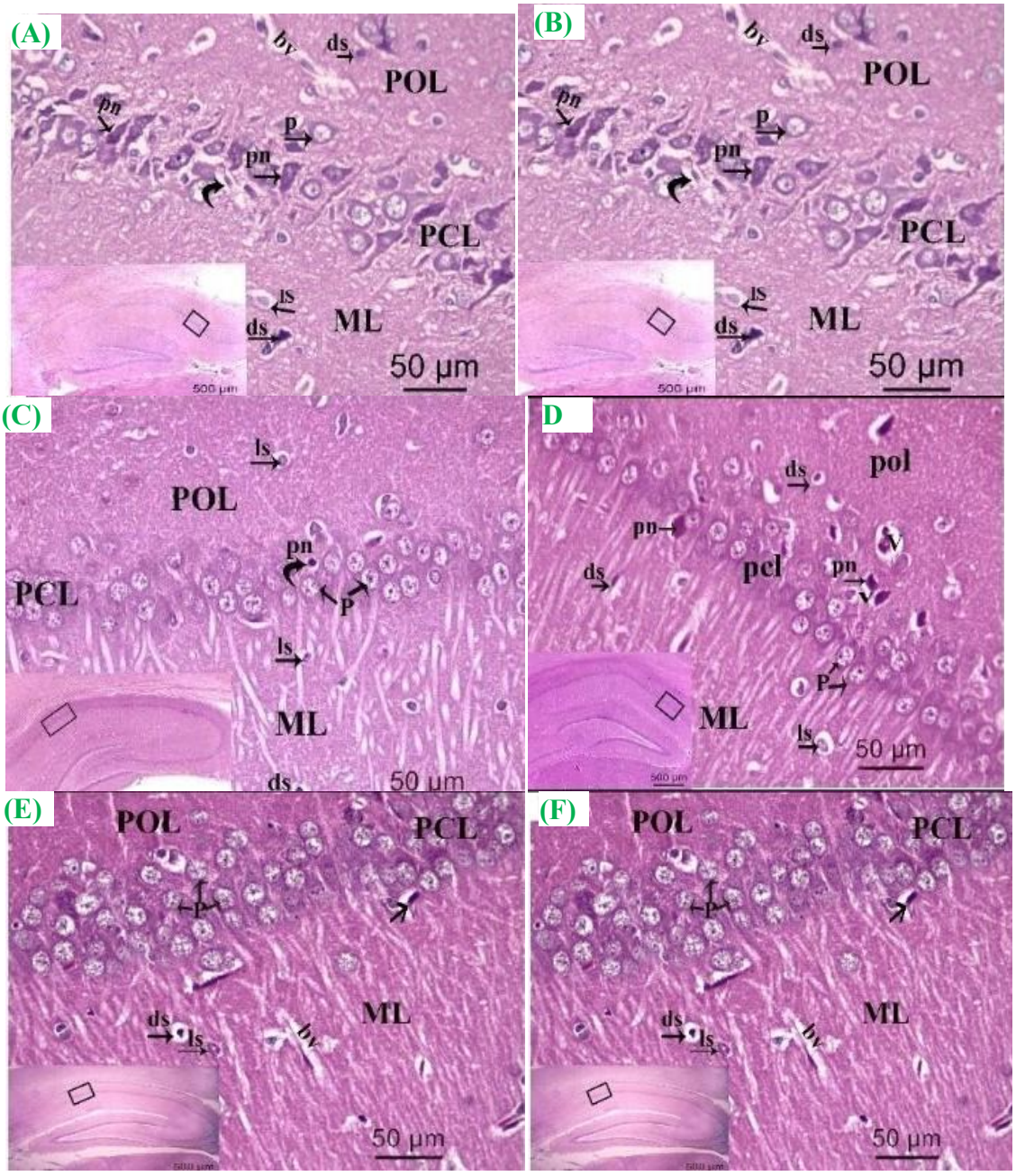

Figure 5: Photomicrographs of H&E-stained hippocampal CA1 region (high magnification, ×400; scale bar = 50 µm) in Control (A), Alloxan + $HgCl_2$ (B), Alloxan + $HgCl_2$ + *Chromolaena odorata* extract 200 mg/kg (C), Alloxan + $HgCl_2$ + *Chromolaena odorata* extract 400 mg/kg (D), Alloxan + $HgCl_2$ + *Chromolaena odorata* extract 600 mg/kg (E), and Alloxan + $HgCl_2$ + Metformin (F). Group B exhibited neuronal degeneration and cellular disorganization, whereas treatment groups showed improved neuronal integrity.

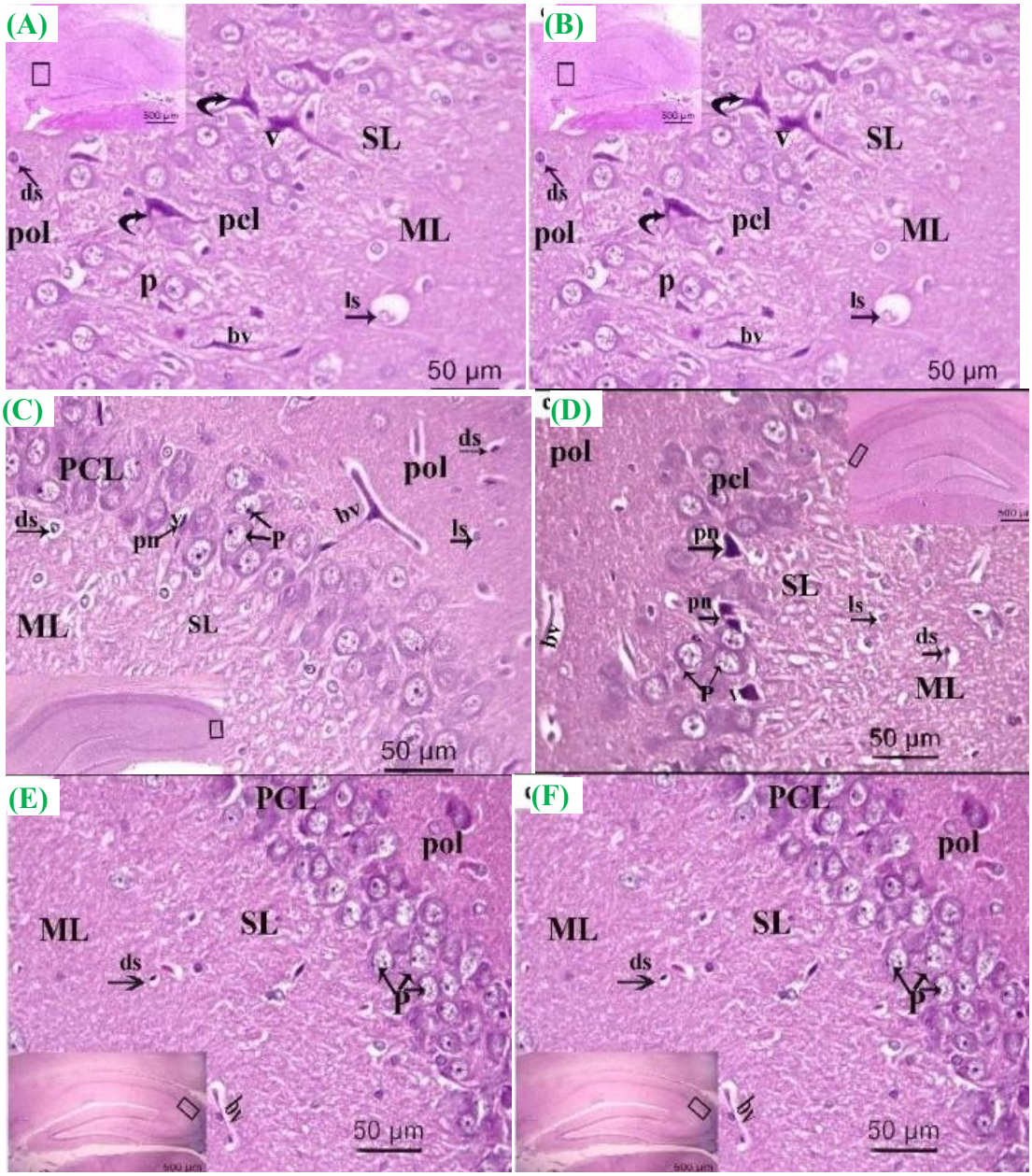

Figure 6: Photomicrographs of H&E-stained hippocampal sections of CA3 region (high magnification, ×400; scale bar = 50 µm) in Control (A), Alloxan + $HgCl_2$ (B), Diabetic + $HgCl_2$ + *Chromolaena odorata* extract 200 mg/kg (C), Alloxan + $HgCl_2$ + *Chromolaena odorata* extract 400 mg/kg (D), Alloxan + $HgCl_2$ + *Chromolaena odorata* extract 600 mg/kg (E), and Alloxan + $HgCl_2$ + Metformin (F). Group B showed marked neuronal damage, while treatment groups demonstrated preservation of hippocampal cytoarchitecture.

Effect of *Chromolaena odorata* on astrocyte activation

The GFAP immunoreactivity of CA1 and CA3 of normal control (a, b) showed astrocytes with thin short processes among pyramidal cells, group B (c, d) displayed many astrocytes with multiple thick long arrows among the pyramidal cells, group C (e, f) has some astrocytes with thin and thick processes among the pyramidal cells, group D (g, h) revealed astrocytes with thin ramified processes among pyramidal cells, and groups E (i, j), and F presented astrocytes with thin short processes among the pyramidal cells.

Effect of *Chromolaena odorata* on p53 expression

The p53 Immunoreactivity of CA1 and CA3 of normal control (a, b) showed negative reaction of pyramidal cells, group B (c, d) presented strong positive immunoreactivity in the cytoplasm of most pyramidal cells, group C (e, f) demonstrated positive reaction in the cytoplasm of some pyramidal cells, group D (g, h) displayed positive immunoreactivity (arrow) in the cytoplasm of few pyramidal cells, and group E (i, j) showed negative reaction in most pyramidal cells. Group F showed astrocytes with thin, short processes among the pyramidal cells.

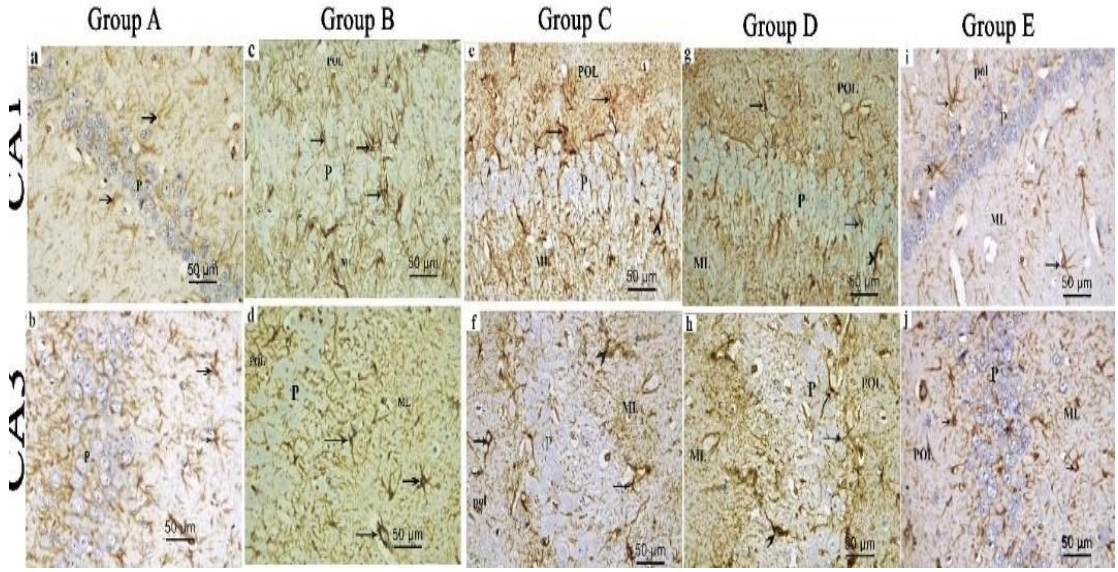

Figure 7: Photomicrographs of GFAP-immunostained hippocampal sections showing astrocyte activation in the CA1 and CA3 regions of Control (A), Diabetic + $HgCl_2$ (B), Diabetic + $HgCl_2$ + *Chromolaena odorata* extract 200 mg/kg (C), Diabetic + $HgCl_2$ + *Chromolaena odorata* extract 400 mg/kg (D), Diabetic + $HgCl_2$ + *Chromolaena odorata* extract 600 mg/kg (E) (×400; scale bar = 50 µm). Group A showed sparse GFAP-positive astrocytes with thin cytoplasmic processes, while group B showed increased GFAP immunoreactivity and reactive gliosis, whereas treatment groups exhibited reduced astrocyte activation in a dose-dependent manner.

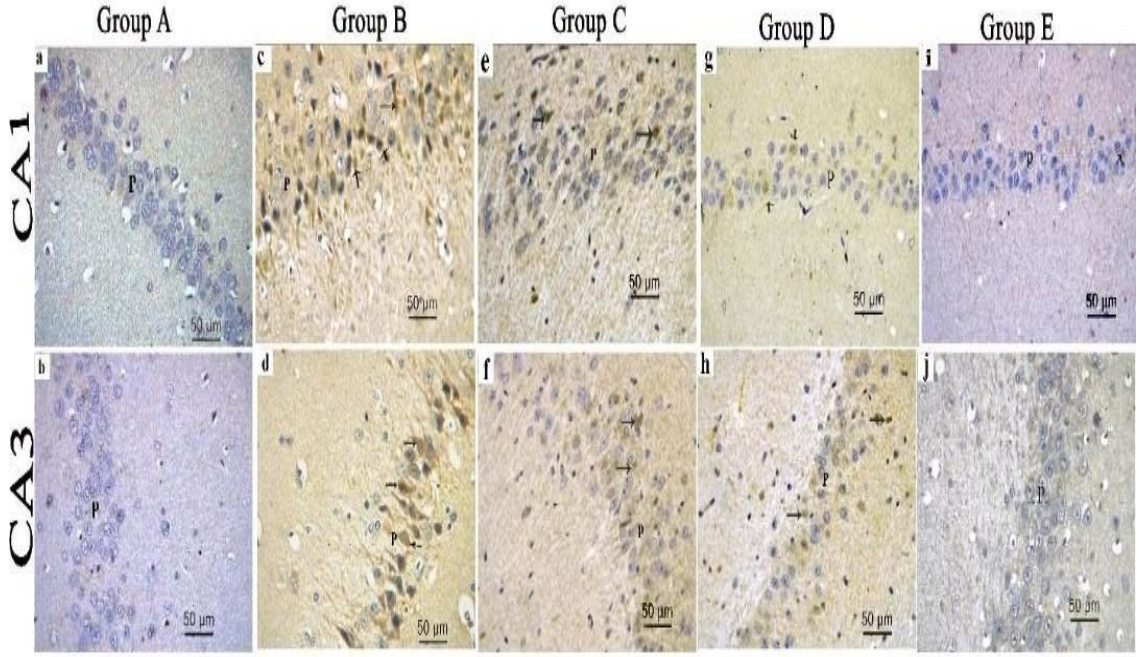

Figure 8: Photomicrographs of p53-immunostained hippocampal sections showing neuronal apoptosis in the CA1 and CA3 regions of Control (A), Diabetic + $HgCl_2$ (B), Diabetic + $HgCl_2$ + *Chromolaena odorata* extract 200 mg/kg (C), Diabetic + $HgCl_2$ + *Chromolaena odorata* extract 400 mg/kg (D), Diabetic + $HgCl_2$ + *Chromolaena odorata* extract 600 mg/kg (E)(×400; scale bar = 50 µm). Control showed negative or minimal p53 expression, while group B showed increased p53 immunoreactivity, whereas treatment groups exhibited reduced p53 expression in a dose-dependent manner.

DISCUSSION

The marked elevation in malondialdehyde level accompanied by decreased superoxide dismutase and glutathione peroxidase activities in untreated diabetic rats exposed to inorganic mercury indicates severe oxidative stress and lipid peroxidation in the hippocampal tissue. These findings suggest that combined hyperglycemia and mercury toxicity enhanced reactive oxygen species generation, leading to oxidative neuronal injury. Similar observations have been reported in previous studies demonstrating that excessive ROS production contributes to mitochondrial dysfunction, neuronal membrane damage, and neurodegeneration in diabetic and toxicological conditions [19, 20].

The reduction in endogenous antioxidant enzymes further indicates impairment of cellular antioxidant defense mechanisms, thereby increasing tissue susceptibility to oxidative injury. Antioxidant enzymes play important roles in detoxifying reactive oxygen species, and their depletion predisposes tissues to oxidative damage [23]. Previous investigations have similarly shown that chronic hyperglycemia suppresses antioxidant enzyme activity and promotes neuronal degeneration in the hippocampus [21, 22].

The administration of *Chromolaena odorata* extract significantly reduced MDA levels while improving SOD and GPx activities across the treated groups. This suggests that the extract possesses potent antioxidant activity capable of restoring cellular redox balance and limiting oxidative damage. The observed protective effect is attributed to flavonoids and phenolic compounds of *Chromolaena odorata,* which are known to scavenge free radicals and enhance endogenous antioxidant defenses [24, 26]. Similar studies have demonstrated that plant-derived antioxidants protect neuronal tissues against oxidative stress-mediated injury by improving antioxidant enzyme activities and reducing lipid peroxidation [25].

Histopathological examination of the hippocampus in untreated diabetic rats exposed to mercury revealed marked neuronal degeneration, disrupted pyramidal cell arrangement, vacuolation, and distortion of normal hippocampal cytoarchitecture within the CA1, CA3, and dentate gyrus regions. These findings indicate severe neuronal injury resulting from the combined effects of hyperglycemia and mercury toxicity. Previous reports have associated diabetes-induced oxidative stress with structural alterations in hippocampal neurons and impairment of cognitive function [27, 28]. Similarly, inorganic mercury exposure has been shown to induce neuronal degeneration and disruption of brain histoarchitecture through oxidative and inflammatory mechanisms [29, 30]. The severe hippocampal alterations observed reflect synergistic neurotoxic effects of diabetes and mercury exposure.

The treatment with *Chromolaena odorata* extract improved hippocampal architecture in a dose-dependent manner, as evidenced by the preservation of pyramidal neurons, reduced vacuolation, and restoration of normal neuronal arrangement. The histological improvements correspond to the observed reduction in oxidative stress markers, suggesting that the neuroprotective effects of the extract are achieved by its antioxidant and anti-inflammatory properties. Similarly, the neuroprotective effect of flavonoid-rich medicinal plants was reported in experimental models of oxidative neuronal injury [24, 31]. The near-normal histological appearance observed in the higher-dose treatment groups further supports the therapeutic potential of the extract in protecting hippocampal neurons against metabolic and toxic insults.

The intense GFAP immunoreactivity observed in the untreated group indicates marked astrocyte activation and reactive astrogliosis within the hippocampus following combined diabetes and mercury exposure. Astrocyte activation is a well-recognized response to neuronal injury and neuroinflammation within the central nervous system [33]. Previous studies have shown that both hyperglycemia and mercury toxicity promote oxidative stress and inflammatory responses capable of inducing astrocytic activation and glial proliferation in brain tissues [32, 35]. The increased GFAP immunoreactivity observed in this study, therefore, suggests significant neuroinflammatory changes associated with hippocampal injury.

However, treatment with *Chromolaena odorata* extract resulted in reduced GFAP immunoreactivity and improvement in astrocytic morphology across the treated groups. This finding suggests attenuation of neuroinflammation and suppression of reactive astrogliosis, likely secondary to a reduction in oxidative stress. Previous investigations have similarly demonstrated that antioxidant therapies may reduce astrocyte activation and restore normal neuronal microenvironment in neurodegenerative conditions [24, 34].

The increased p53 immunoreactivity observed in untreated diabetic rats exposed to mercury indicates activation of apoptotic pathways in response to oxidative stress and cellular injury. The p53 plays an important role in regulating apoptosis resulting from DNA damage and oxidative stress. Previous studies have shown that excessive ROS generation activates p53 signaling pathways, leading to neuronal apoptosis and progressive neurodegeneration [36, 37]. Mercury-induced oxidative stress has also been associated with p53-dependent apoptotic mechanisms in neural tissues [38]. The marked p53 expression observed in this study, therefore, suggests increased neuronal apoptosis within the

hippocampus following combined diabetic and mercury-induced injury.

Following treatment with *Chromolaena odorata* extract, p53 immunoreactivity was markedly reduced in the treated groups, indicating suppression of apoptosis and improved neuronal survival. This anti-apoptotic effect may be related to the antioxidant properties of the extract, which likely reduced oxidative stress and stabilized cellular redox balance. Similar findings have demonstrated that flavonoid-rich plant extracts protect neurons against oxidative stress-induced apoptosis through modulation of apoptotic signaling pathways [6, 39]. Collectively, these findings support the neuroprotective potential of *Chromolaena odorata* against hippocampal damage induced by diabetes and mercury toxicity.

CONCLUSION

Ethanol leaf extract of *Chromolaena odorata* demonstrated significant ameliorative effects against hippocampal damage induced by alloxan-induced diabetes and mercuric chloride exposure. The extract reduced oxidative stress, inflammation, astrocyte activation, and neuronal apoptosis while improving hippocampal cytoarchitecture.

Conflict of interest: The Authors have no conflict of interest to declare

Author's Contribution: CMN: Research Conception, design, data acquisition, and collection, drafting and revising the Manuscript; NCO: research supervision; AEN: review of study and manuscript; AIM: laboratory work; data collection and analysis; UVU: research conception and design.

REFERENCES

1. American Diabetes Association. 2. Classification and diagnosis of diabetes: standards of medical care in diabetes-2023. Diabetes Care. 2023;46(Suppl 1):S19-S40. doi:10.2337/dc23-S002
2. International Diabetes Federation. IDF diabetes atlas. 10th ed. Brussels: International Diabetes Federation; 2021.
3. Forbes JM, Cooper ME. Mechanisms of diabetic complications. Physiol Rev. 2013;93(1):137-188. doi:10.1152/physrev.00045.2011
4. Biessels GJ, Despa F. Cognitive decline and dementia in diabetes mellitus: mechanisms and clinical implications. Nat Rev Endocrinol. 2018;14(10):591-604. doi:10.1038/s41574-018-0048-7
5. Lenzen S. The mechanisms of alloxan- and streptozotocin-induced diabetes. Diabetologia. 2008;51(2):216-226. doi:10.1007/s00125-007-0886-7
6. Sies H, Jones DP. Reactive oxygen species (ROS) as pleiotropic physiological signalling agents. Nat Rev Mol Cell Biol. 2020;21(7):363-383. doi:10.1038/s41580-020-0230-3
7. Brownlee M. Biochemistry and molecular cell biology of diabetic complications. Nature. 2001;414(6865):813-820. doi:10.1038/414813a
8. Eichenbaum H. The role of the hippocampus in memory and cognition. Nat Rev Neurosci. 2021;22(8):487-502. doi:10.1038/s41583-021-00482-6
9. Rice KM, Walker EM, Wu M, Gillette C, Blough ER. Environmental mercury and its toxic effects. J Prev Med Public Health. 2014;47(2):74-83. doi:10.3961/jpmph.2014.47.2.74
10. Farina M, Rocha JBT, Aschner M. Mechanisms of mercury-induced neurotoxicity: evidence from experimental studies. Toxicology. 2019;408:1-12. doi:10.1016/j.tox.2019.06.004
11. Yee S, Choi BH. Oxidative stress in neurotoxic effects of methylmercury poisoning. Neurotoxicology. 1996;17(1):17-26.
12. World Health Organization. WHO traditional medicine strategy 2022-2027. Geneva: World Health Organization; 2022.
13. Omokhua AG, McGaw LJ, Finnie JF, van Staden J. *Chromolaena odorata* (L.) R.M. King & H. Rob. (Asteraceae) in sub-Saharan Africa: a synthesis and review of its medicinal potential. J Ethnopharmacol. 2016;183:112-122. doi:10.1016/j.jep.2015.04.057
14. Akinmoladun AC, Ibukun EO, Afor E, Obuotor EM, Farombi EO. Phytochemical constituents and antioxidant activity of *Chromolaena odorata*. J Med Plants Res. 2020;14(6):245-252.
15. Ngono Ngane A, Ebelle Etame R, Dibong S. Phytochemical composition and pharmacological activities of *Chromolaena odorata*: a review. J Ethnopharmacol. 2021;268:113610. doi:10.1016/j.jep.2020.113610
16. Ikewuchi CC, Ikewuchi JC, Ifeanacho MO. Hypoglycemic activity of *Chromolaena odorata* leaf extract in alloxan-induced diabetic rats. J Med Plants Res. 2014;8(8):412-420.
17. Rena G, Hardie DG, Pearson ER. The mechanisms of action of metformin. Diabetologia. 2017;60(9):1577-1585. doi:10.1007/s00125-017-4342-z
18. Suvarna SK, Layton C, Bancroft JD. Bancroft's theory and practice of

histological techniques. 8th ed. Elsevier; 2018.
19. Xu S, Gao Z, Jiang L, Li J, Qin Y, Zhang D, *et al*. High glucose- or AGE-induced oxidative stress inhibits hippocampal neuronal mitophagy through the Keap1-Nrf2-PHB2 pathway in diabetic encephalopathy. Sci Rep. 2024;14(1):24044. doi:10.1038/s41598-024-75000-0
20. Butterfield DA, Lauderback CM. Lipid peroxidation and protein oxidation in Alzheimer's disease brain: potential causes and consequences involving amyloid beta-peptide-associated free radical oxidative stress. Free Radic Biol Med. 2002;32(11):1050-1060. doi:10.1016/s0891-5849(02)00794-3
21. Valko M, Rhodes CJ, Moncol J, Izakovic M, Mazur M. Free radicals, metals and antioxidants in oxidative stress-induced cancer. Chem Biol Interact. 2006;160(1):1-40. doi:10.1016/j.cbi.2005.12.009
22. Maciejczyk M, Żebrowska E, Chabowski A. Insulin resistance and oxidative stress in the brain: what's new? Int J Mol Sci. 2019;20(4):874. doi:10.3390/ijms20040874
23. Halliwell B, Gutteridge JMC. Free radicals in biology and medicine. 5th ed. Oxford University Press; 2015.
24. Farombi EO, Owoeye O. Antioxidative properties of *Chromolaena odorata*. Int J Environ Res Public Health. 2011;8(6):2533-2555. doi:10.3390/ijerph8062533
25. Oyovwi MO, Chijiokwu EA, Ben-Azu B, Atere AD, Joseph UG, Ogbutor UG, *et al*. Potential roles of natural antioxidants in modulating neurodegenerative disease pathways. Mol Neurobiol. 2025;62(8):10367-10397. doi:10.1007/s12035-025-04578-3
26. Akinmoladun AC, Ibukun EO, Afor E, Obuotor EM, Farombi EO. Antioxidant activity of *Chromolaena odorata*. Afr J Biotechnol. 2007;6(10):1197-1201.
27. Biessels GJ, Reagan LP. Hippocampal insulin resistance and cognitive dysfunction. Nat Rev Neurosci. 2015;16(11):660-671. doi:10.1038/nrn4019
28. Sutherland RJ, McDonald RJ, Savage DD. Learning and memory deficits associated with diabetes. Neurosci Biobehav Rev. 2004;28(4):507-514. doi:10.1016/j.neubiorev.2004.09.002
29. Farina M, Rocha JBT, Aschner M. Methylmercury-induced neurotoxicity. Life Sci. 2011;89(15-16):555-563. doi:10.1016/j.lfs.2011.05.020
30. Aschner M, Syversen T, Souza DO, Rocha JBT, Farina M. Involvement of glutamate and reactive oxygen species in methylmercury neurotoxicity. Braz J Med Biol Res. 2007;40(3):285-291. doi:10.1590/S0100-879X2007000300001
31. Hernández-Cruz EY, Eugenio-Pérez D, Ramírez-Magaña KJ, Pedraza-Chaverri J. Effects of vegetal extracts and metabolites against oxidative stress and associated diseases: studies in Caenorhabditis elegans. ACS Omega. 2023;8(10):8936-8959. doi:10.1021/acsomega.2c07885
32. Lee KS, Yoon SH, Hwang I, Ma JH, Yang E, Kim RH, *et al*. Hyperglycemia enhances brain susceptibility to lipopolysaccharide-induced neuroinflammation via astrocyte reprogramming. J Neuroinflammation. 2024;21(1):137. doi:10.1186/s12974-024-03123-6
33. Pekny M, Nilsson M. Astrocyte activation and reactive gliosis. Glia. 2005;50(4):427-434. doi:10.1002/glia.20207
34. Wang X, Wang Q, Cai Z, Ni C, Wang H, Liu H, *et al*. Knockdown of PDPN in astrocytes reduces hippocampal inflammation in T2DM mice. Front Immunol. 2025;16:1503807. doi:10.3389/fimmu.2025.1503807
35. Aschner M, Syversen T, Souza DO, Rocha JBT, Farina M. Glutamate and reactive oxygen species in methylmercury neurotoxicity. Braz J Med Biol Res. 2007;40(3):285-291. doi:10.1590/S0100-879X2007000300001
36. Levine AJ, Oren M. The first 30 years of p53: growing ever more complex. Nat Rev Cancer. 2009;9(10):749-758. doi:10.1038/nrc2723
37. Vousden KH, Prives C. Blinded by the light: the growing complexity of p53. Cell. 2009;137(3):413-431. doi:10.1016/j.cell.2009.04.037
38. Ghosh D, Das UB, Misro M, Ghosh S. Mercury-induced oxidative stress and apoptosis. Toxicol Lett. 2008;182(1-3):12-18. doi:10.1016/j.toxlet.2008.08.003
39. Wang S, Liu A, Xu C, Hou J, Hong J. GLP-1(7-36) protected against oxidative damage and neuronal apoptosis in the hippocampal CA region after traumatic brain injury by regulating ERK5/CREB. Mol Biol Rep. 2024;51(1). doi:10.1007/s11033-024-09239-3